



Scanning tunneling spectroscopy and density functional calculation of silicon dangling bonds on the Si(100)-2 × 1:H surface

Wei Ye^{a,b,*}, Kyoungmin Min^{a,d}, Pamela Peña Martin^b, Angus A. Rockett^b,
N.R. Aluru^{a,d}, Joseph W. Lyding^{a,b,c}

^a Beckman Institute for Advanced Science and Technology, University of Illinois at Urbana–Champaign, Urbana, IL 61801, United States

^b Department of Materials Science and Engineering, University of Illinois at Urbana–Champaign, Urbana, IL 61801, United States

^c Department of Electrical and computer Engineering, University of Illinois at Urbana–Champaign, Urbana, IL 61801, United States

^d Department of Mechanical Science and Engineering, University of Illinois at Urbana–Champaign, Urbana, IL 61801, United States

ARTICLE INFO

Article history:

Received 13 October 2012

Accepted 29 November 2012

Available online 7 December 2012

Keywords:

UHV-STM

Silicon dangling bond

Density functional calculations

Scanning tunneling spectroscopy

Hydrogen passivated silicon

Si(100) surface

Dangling bond wire

ABSTRACT

We studied electronic properties of atomic-scale dangling bond (DB) and DB wires on Si(100)-2 × 1:H surfaces using a ultrahigh vacuum scanning tunneling microscope (UHV-STM). The decay of the near-midgap DB-states induced by an unpaired DB depends on the crystalline orientation of the Si(100) surface. The decay length of the DB-states of an unpaired DB wire can be ~2.5 nm along the dimer row direction. The perturbation from an unpaired DB to an adjacent paired DB is also demonstrated. The results are in good agreement with density functional calculations.

© 2012 Elsevier B.V. All rights reserved.

1. Introduction

Silicon dangling bonds (DBs) are common defects observed on the Si(100) surface. The DB states induced within the bandgap of Si are responsible for the Fermi level pinning at the surface [1]. It has been shown that by using an ultrahigh vacuum (UHV) scanning tunneling microscope (STM), one can selectively pattern silicon (Si) dangling bonds (DBs) with atomic level precision on the hydrogen-passivated Si(100) surface [2–4]. For example, an atomic wire can be formed on the H-Si(100) surface by removing hydrogen atom by atom using the STM tip along a Si dimer row. Due to the coupling of the DB states in the wire, the unpaired DB wire shows one-dimensional metallic behavior, which could be used as an atomic size interconnect [5]. In addition, charged DBs can serve as atomic scale quantum dots (QDs) [6–8] leading to the construction of a room temperature quantum-dot cellular automata (QCA) cell [6]. Furthermore, Si DB patterns can also be used as templates for subsequent selective chemistry due to the difference in reactivity between bare and hydrogen passivated silicon [9]. The potential applications to

atomic-scale electronic devices arouse an increased interest in the study of Si DBs.

Understanding the electronic properties of silicon DBs is essential for their integration into future atomic scale electronics. Piva et al. [6] demonstrated by STM that a negatively charged unpaired DB can electrostatically perturb the *I-V* characteristics of a nearby styrene molecular wire. Recently, Raza et al. [10] studied the same case theoretically and proposed that the unpaired DB can introduce a near-midgap state in the local density of states (LDOS) of neighboring Si atoms. The DB-induced gap states (DBIGS) can have an additional electronic contribution to the perturbation within a 1 nm region. Thus the decay of the near-midgap DB state of an unpaired DB has the potential to engineer the electronic properties of nearby atomic scale devices. However, further experimental evidence of this behavior is lacking.

In this study, we use UHV-STM and Spanish Initiative for Electronic Simulations with Thousands of Atom (SIESTA) calculations to investigate the decay of DBIGS from unpaired DBs and unpaired DB wires. We also demonstrate the perturbations from an unpaired DB upon a paired DB within 1 nm.

2. Experimental methods

The silicon used in this study is boron doped Si(100) which has a resistivity of 0.01–0.02 Ω · cm. The hydrogen passivated Si(100)-2 × 1 surface was prepared by first degassing in UHV in the preparation

* Corresponding author at: Department of Materials Science and Engineering, University of Illinois at Urbana–Champaign, Urbana, IL 61801, United States. Tel.: +1 408 875 6836.

E-mail address: weiyuiuc@gmail.com (W. Ye).

chamber at 600 °C overnight. The Si sample was subsequently flashed to ~1200 °C several times to form the clean Si(100)-2×1 surface. Finally, the reconstructed silicon sample was exposed to atomic hydrogen at 377 °C to ensure a hydrogen passivated surface with monohydride coverage [2].

The STM experimental data were collected within a homebuilt UHV-STM [11] with a base pressure of approximately 7×10^{-11} Torr. Electrochemically etched polycrystalline tungsten tips were used. In our experimental setup, the tip is grounded through a current preamplifier and the bias voltage is applied to the sample. STM images were acquired in constant current mode, with a typical setpoint tunneling current of 50 pA. Individual DB patterns were created by the feedback control lithography (FCL) method [4]. The feedback loop immediately terminates patterning once a hydrogen desorbing event is detected. DB wires were fabricated by repeatedly using FCL to make a row of DBs. Scanning tunneling spectroscopy (STS) is conducted by collecting tunneling current–voltage (I – V) spectra at user defined locations within the scan window. The tip is held at those locations with the feedback loop temporarily disabled. Tunneling current is recorded while sweeping sample bias from -2.0 V to $+2.0$ V. All the experiments were carried out at room temperature.

3. Theoretical methods

To explore the electronic properties and compare them with experimental results of the effect of the Si DBs on the silicon surface, we performed SIESTA calculations based on fully self-consistent density functional theory (DFT) methods [12]. A generalized gradient approximation (GGA) [13] with revised Perdew–Burke–Ernzerhof (RPBE) is implemented for the parameterization of the exchange–correlation functional [14]. The core electrons are replaced by the norm-conserving pseudopotentials [15] and a double zeta basis plus polarization (DZP) numerical atomic orbital is employed. A mesh cutoff of 400 Ry is used. The number of k-points is generated with $7 \times 7 \times 1$ Monkhorst–Pack for the structural relaxation and $10 \times 10 \times 1$ Monkhorst–Pack for the band structure calculation [16].

We constructed a 5 layer Si(100)-(2×1) unit cell for the unpaired DB and unpaired DB wire case, and use 13 layers for the paired DB and paired plus unpaired DB case. The bulk structure with a 6×3 unit cell for each different layer is optimized until the maximum residual force is less than 0.01 eV/Å. Finally, we set up several DB configurations using the unit cell for each case and computed the band structure and LDOS. The band structure is computed at the highest symmetrical direction on the surface Brillouin zone of silicon. Additional structural optimizations after creating DBs are not considered due to their negligible effect on the band structure, except for the cases of paired DBs, and paired and unpaired DBs [17]. For both cases, structures are relaxed until the maximum force is less than 0.05 eV/Å. After structural optimization, silicon dimer length is obtained as 2.328 Å with a buckling angle of 17.95°, which shows the reasonable agreement with the previous work [18]. Detailed information for each different DB state is shown in Table 1. DBs are created as the same way in the STM experiments.

Table 1
Details of unit cell setup.

Unit cell construction	Unit cell	Number of atoms
Unpaired DB	10×9	450
Unpaired wire DBs ^a	6×15	660
Unpaired wire DBs ^b	12×6	528
Paired DBs	8×6	624
Paired and Unpaired DBs	8×6	624

^aAlong and ^bacross the Si dimer row direction. Number of atoms is silicon atoms only. Periodic boundary conditions for both of x and y-direction are applied for all cases—except for unpaired wire DBs^a—along the dimer direction and unpaired wire DBs^b—across dimer direction. Edges are terminated with hydrogens for those cases.

4. Results and discussion

Fig. 1a shows a filled-state STM image of an unpaired silicon DB fabricated by STM on the Si(100)-2×1:H surface. The unpaired DB appears as a bright protrusion in the filled-state image due to its enhanced LDOS. The bright feature appears off-center on the dimer row, indicating that only one hydrogen was desorbed from a Si dimer and an unpaired DB was formed. To investigate the electronic properties of the unpaired DB, we took current–voltage (I – V) spectra across the DB at each pixel along a line. Fig. 1c shows the Log I – V spectra map taken along the Si dimer row direction. The position along the dimer row direction is represented on the horizontal axis, the applied sample bias plotted on the vertical axis, and the log I value is color-mapped onto the plane. The unpaired DB has finite local density of states (LDOS) at the Fermi level while the Si substrate ~2 nm away from the DB shows a semiconducting band gap of 1.10 eV. However, the electronic property of the Si within ~2 nm from the center of the unpaired DB is changed by the decay of DBIGS. The lengths of the decay regions are 1.91 nm to the left and 1.65 nm to the right, as shown in Fig. 1c. The DB switched position to the right Si atom in the same Si dimer after recording several sets of spectra data. The topographic image is shown in Fig. 1b. The hydrogen atom intradimer diffusion under the field of the STM tip at room temperature has been observed before [19]. Fig. 1d shows a log I – V spectra map in the direction perpendicular to the Si dimer rows. The decay regions are 1.37 nm and 1.16 nm to the left and right of the DB respectively, and are around 30% smaller than those along the dimer row directions. This is because the Si dimers along the dimer row direction have a close proximity of 3.84 Å, while the separation between dimers across the dimer row direction is 7.68 Å. Thus the DB state of the unpaired DB can decay further into the Si lattice along the dimer row direction.

Fig. 1e shows the LDOS plot of an unpaired DB and the Si substrate. The unpaired DB shows finite (non-zero) LDOS throughout the band gap of the Si substrate and has a peak at 0.74 eV. It has been shown that the near midgap state for the case of an unpaired DB is very flat [17], and this has also been observed in the calculations. Therefore, we implement DFT-molecular dynamics (MD) simulations to study the effect of finite temperature to compare with the experimental result. Coordinates of each step at 300 K from DFT-MD are obtained to compute the band structure, and the locations of near midgap states are measured to be around 0.363 eV, showing the thermal broadening effect at finite temperature. Simulation results of LDOS of DB state along and across Si dimer row direction are shown in Fig. 1f and g respectively and they show a rapid decay of the DB contribution to the near midgap state in LDOS. The DB state finally disappears at 1.54 nm from the DB center along the dimer row direction. As for the across dimer row direction, the transition regions are 1.32 nm and 1.0 nm to the left and right of the DB, respectively, which are in reasonable agreement with experiment. The transition region at 300 K for along dimer row direction is 1.92 nm and it shows smoother decay rate of the LDOS peak due to the DB state than for the ground state case.

By tuning the patterning parameters, we can desorb both hydrogen atoms from the same Si dimer to form a paired DB. Unlike an unpaired DB, a DB pair is imaged at the center of the dimer row in a filled-state image; an example is shown in Fig. 2a. Fig. 2c shows the Log I – V spectra map across the paired DBs. A band gap of 0.90 eV is observed on the paired DBs, while the adjacent Si substrate continues to exhibit a band gap of 1.10 eV. In contrast to the unpaired DB, there is no apparent decay region between the paired DBs and the adjacent Si. The LDOS of the paired DBs, shown in Fig. 2e, consists of two peaks, at -0.30 eV and 1.02 eV. These are from bonding (π) and anti-bonding (π^*) states of the paired DBs. Compared to the Si substrate, the π^* state is 0.24 eV below the conduction band and the π state is close to the valence band (0.04 eV below). The experimental result is consistent with the calculated band structure of a paired DB,

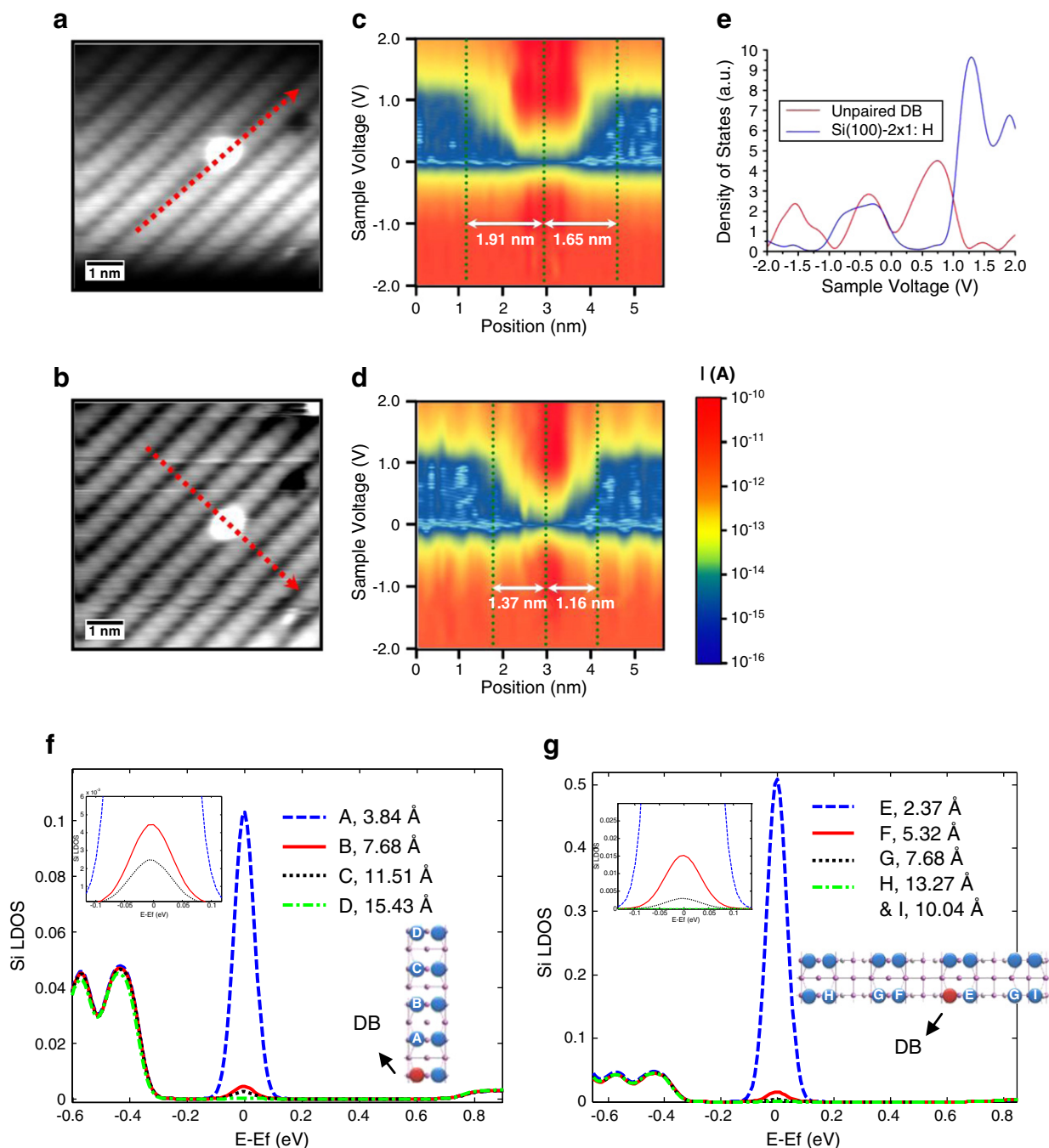


Fig. 1. (a) Filled-state STM image of an unpaired dangling bond on Si(100)-2×1:H surface. ($V_s = -2.0$ V, $I_t = 50$ pA) (b) STM image of the DB in the same Si dimer after switching position from left to right. (c,d) Log I - V spectra plotted as a function of position in (c) for the unpaired DB in (a) and in (d) for the DB in (b). Red dotted arrows in (a) and (b) denote where the I - V spectra maps were taken. The green dotted lines in (c) and (d) are used to highlight the positions of the center of the unpaired DB and where the Si bandgap is fully recovered. (e) DOS- V spectra of the unpaired DB in (a) and silicon substrate. (f) Simulated LDOS of Si atoms along the Si dimer direction with the distance from DB. (Inset shows the magnified view for atoms B,C, and D.) (g) Simulated LDOS of Si atoms across the Si dimer direction with the distance from DB. (Inset shows the magnified view for atoms F,G,H, and I).

which is shown in Fig. 2f, which shows that the π^* state is 0.20 eV below the conduction band and the π state is close to the valence band (0.09 eV below). To study the interaction between a paired and an unpaired DB, we introduce a DB cluster 1.8 nm away from the paired DB in Fig. 2a. The topographic image is shown in Fig. 2b. The DB cluster consists of a paired DB and an unpaired DB next to it. The unpaired DB is 1.9 nm to the right of the paired DB. So the influence from the unpaired DB on the left paired DB is negligible. However, the distance between the right paired DB and the unpaired DB is only 0.66 nm. We expect a strong interaction between these two DBs. Fig. 2d shows an STS spectra map across both paired DBs in the dimer row direction. The left paired

DB shows a band gap of 0.90 eV experimentally, as expected, and 0.91 eV from the simulation. However, the band gap of the right paired DB is reduced to 0.78 eV, or to 0.76 eV by simulation. The LDOS plot in Fig. 2e indicates a shift of the π^* state peak to 0.88 eV. The result is also consistent with the calculated band structure shown in Fig. 2g.

Fig. 3a shows an unpaired DB wire consisting of seven unpaired DBs along the dimer row direction. An additional unpaired DB is formed on the next dimer row due to spurious depassivation. STS spectra maps were taken both along the dimer row direction and across the dimer row direction to reveal the electronic properties of the DB wire. Fig. 3b shows the log I - V spectra map along the dimer

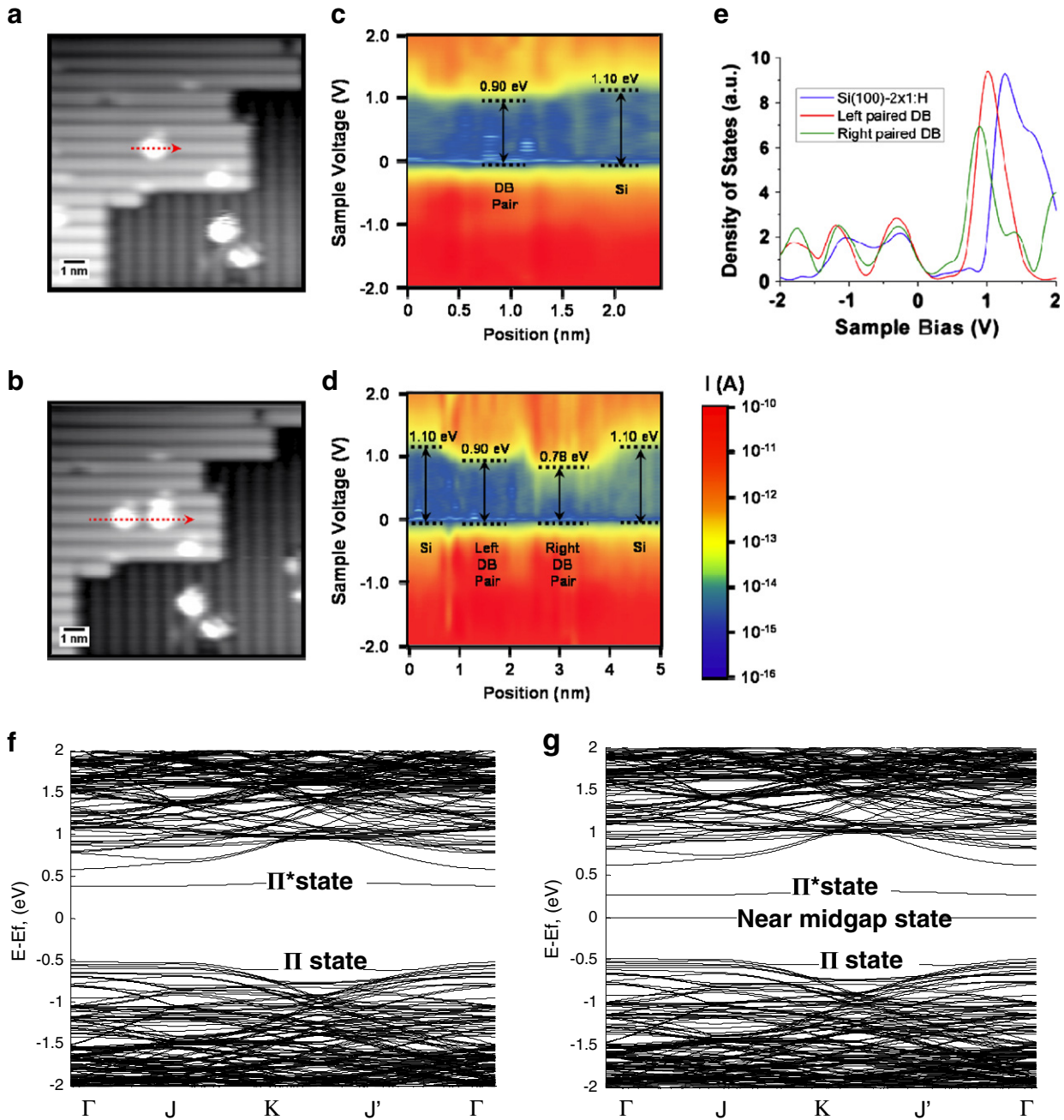


Fig. 2. (a) STM topographic image of a paired DB fabricated by removing two hydrogen atoms from the same Si dimer. (b) STM topographic image of a DB cluster formed to the right of the paired DB in (a). (c) Log I - V spectra map taken on the paired DB, as indicated by the red dotted arrow in (a). (d) Log I - V spectra map taken across both paired DBs in (b) along the red dotted arrow. (e) DOS-V spectrum for both paired DBs and Si substrate in (b). Simulation results are plotted in (f) for the paired DB and (g) for the paired DB and unpaired DB case.

row direction. With strong interaction between the DBs just 3.84 Å away from each other, the whole DB wire exhibits metallic behavior. The decay length of the DB state is much longer than that in the single DB case. The transition region, where the band gap of the Si is reduced due to DB-state induced gap states, is in a range of 2–2.5 nm from the ends of the wire, along the dimer row. However, in the direction perpendicular to the dimer rows, the decay length of the DB states is comparable to the single DB case. As shown in Fig. 3c, the length is about 1.1 nm. Simulation results from studying the LDOS decay of the unpaired DB wire state along and across Si dimer row direction are shown in Fig. 3d, and e respectively. As shown for an unpaired DB, the midgap DB state contribution decays rapidly. The DB state

finally disappears at 1.90 nm for along dimer row and 1.00 nm to the left and 1.32 nm to the right for across dimer row direction from the outermost DB respectively, which shows reasonable agreement with experiment.

5. Conclusions

In summary, we investigated the lateral decay of DB states around an unpaired DB. The decay length is anisotropic on the Si(100) surface. The near-midgap state of an unpaired DB decays ~1.9 nm into adjacent Si atoms along the Si dimer row, while the DB states disappear ~1.4 nm across the Si dimer rows, and simulations agree

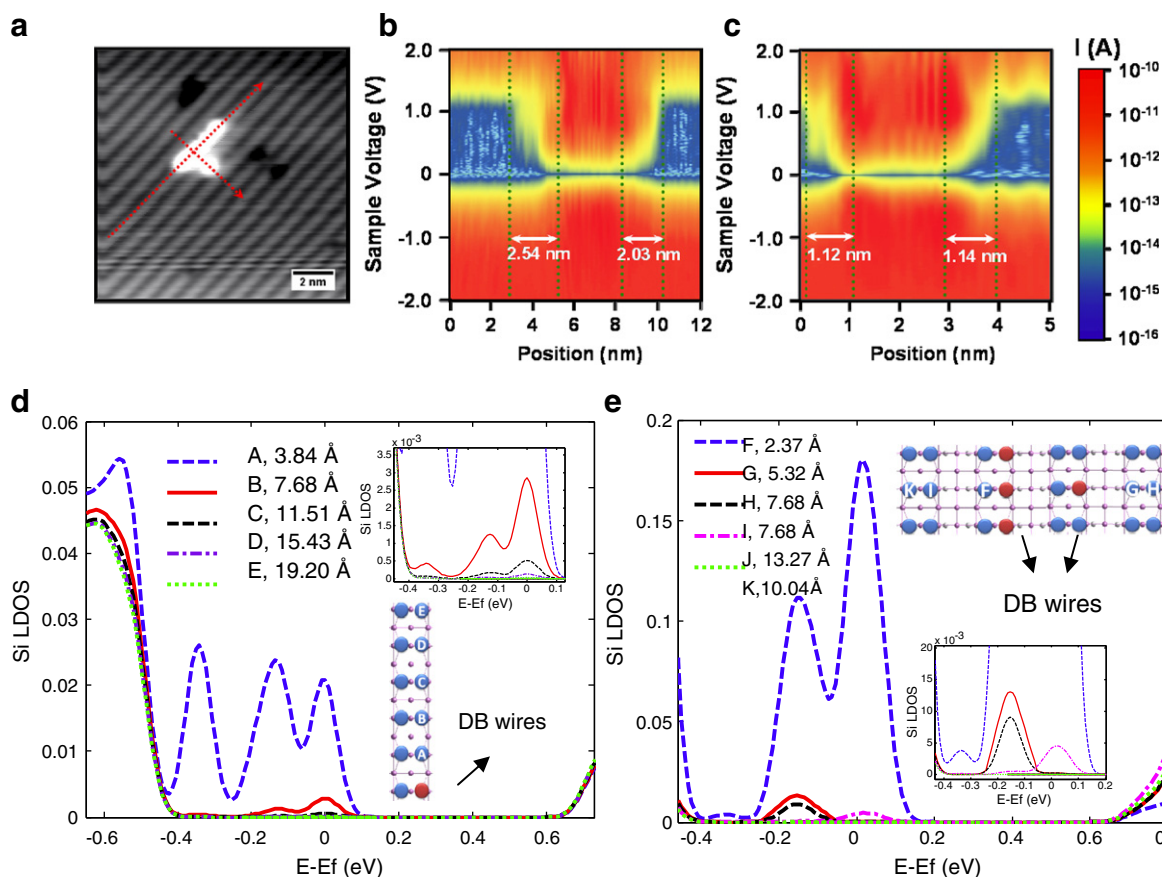


Fig. 3. (a) STM topographic image of an unpaired DB wire along the dimer row direction. The scanning parameters are 50 pA and -2.0 V. Log I - V spectra maps are plotted as a function of position for (b) along the dimer row direction and for (c) perpendicular to the dimer row direction. The dotted red arrows denote where the spectra were taken. (d) Simulated LDOS of Si atoms along the Si dimer direction with the distance from unpaired wire DBs. (Inset shows the magnified view for atoms B, C, D, and E.) (e) Simulated LDOS of Si atoms across the Si dimer direction with the distance from unpaired wire DBs. (Inset shows the magnified view for atoms F, G, H, I, J, and K.)

with these experimental values. With the increasing interactions along the dimer row direction, the decay length of an unpaired DB wire increases to ~ 2.5 nm along the Si dimer row direction, while the decay length in the direction perpendicular to the dimer row is comparable to that of the unpaired DB. We also demonstrated that an unpaired DB can perturb the electronic property of an adjacent paired DB, reducing the bandgap of the paired DB from 0.90 eV to 0.78 eV. Another paired DB 1.9 nm away from the unpaired DB remains unperturbed.

References

- [1] R.J. Hamers, U.K. Kohler, J. Vac. Sci. Technol., A Vac. Surf. Films 7 (4) (1989) 2854.
- [2] J.W. Lyding, T.C. Shen, J.S. Hubacek, J.R. Tucker, G.C. Abeln, Appl. Phys. Lett. 64 (15) (1994) 2010.
- [3] T.C. Shen, C. Wang, G.C. Abeln, J.R. Tucker, J.W. Lyding, P. Avouris, R.E. Walkup, Science 268 (5217) (1995) 1590.
- [4] M.C. Hersam, et al., Nanotechnology 11 (2) (2000) 70.
- [5] T. Hitosugi, T. Hashizume, S. Heike, H. Kajiyama, Y. Wada, S. Watanabe, T. Hasegawa, K. Kitazawa, Appl. Surf. Sci. 130–132 (1998) 340.
- [6] P.G. Piva, G.A. DiLabio, J.L. Pitters, J. Zikovsky, M. d Rezez, S. Dogel, W.A. Hofer, R.A. Wolkow, Nature 435 (7042) (2005) 658.
- [7] M.B. Haider, J.L. Pitters, G.A. DiLabio, L. Livadaru, J.Y. Mutus, R.A. Wolkow, Phys. Rev. Lett. 102 (4) (2009) 046805-4.
- [8] H. Kawai, Y.K. Yeo, M. Saeys, C. Joachim, Phys. Rev. B 81 (19) (2010) 195316.
- [9] M.A. Walsh, M.C. Hersam, Annu. Rev. Phys. Chem. 60 (1) (2009) 193.
- [10] H. Raza, K.H. Bevan, D. Kienle, Phys. Rev. B 77 (3) (2008) 035432.
- [11] J.W. Lyding, S. Skala, J.S. Hubacek, R. Brockenbrough, G. Gammie, Rev. Sci. Instrum. 59 (9) (1988) 1897.
- [12] M.S. José, et al., J. Phys. Condens. Matter 14 (11) (2002) 2745.
- [13] J.P. Perdew, K. Burke, M. Ernzerhof, Phys. Rev. Lett. 77 (18) (1996) 3865.
- [14] B. Hammer, L.B. Hansen, Oslash, J.K. rskov, Phys. Rev. B 59 (11) (1999) 7413.
- [15] N. Troullier, J. Martins, Phys. Rev. B 43 (3) (1993).
- [16] H.J. Monkhorst, J.D. Pack, Phys. Rev. B 13 (12) (1976) 5188.
- [17] H. Raza, Phys. Rev. B 76 (4) (2007) 045308.
- [18] D.Q. Ly, L. Paramonov, C.J. Makatsoris, Phys. Condens. Matter 21 (2009) 185006.
- [19] U.J. Quaade, K. Stokbro, C. Thirstrup, F. Grey, Surf. Sci. 415 (3) (1998) L1037.